Asian Journal of Research and Reviews in Physics

5(1): 33-42, 2021; Article no.AJR2P.73049
ISSN: 2582-5992

Numerical Study of Transparent Conductive Oxide (TCO) Layer on the Performance of Methyl-Ammonium Tin Iodide ($CH_3NH_3SnI_3$) Perovskite Solar Cells Using SCAPS

Faruk Sani[1*] and S. Abdullahi[1]

[1]Department of Physics, Usmanu Danfodiyo University, Sokoto, Nigeria.

Authors' contributions

This work was carried out in collaboration between both authors. Both authors read and approved the final manuscript.

Article Information

DOI: 10.9734/AJR2P/2021/v5i130156
Editor(s):
(1) Prof. Shi-Hai Dong, National Polytechnic Institute, Mexico.
Reviewers:
(1) Yameen Ahmed, Central South University, China.
(2) Divya Jyoti Chawla, Punjabi University, India.
Complete Peer review History: https://www.sdiarticle4.com/review-history/73049

Original Research Article

Received 12 July 2021
Accepted 22 September 2021
Published 30 September 2021

ABSTRACT

Substrates used in perovskite solar cells as front contact are usually transparent conductive oxide (TCO) to allow light to pass through the device. The dominating TCO employed in perovskite solar cells are indium-doped tin oxide (ITO) and fluorine-doped tin oxide (FTO). However, it is imperative to investigate alternative TCOs due to the scarcity of indium metal, relatively low electrical conductivity and high leakage current in ITO and FTO. In this study, simulation has been carried out using Solar Capacitance Simulator (SCAPS) to investigate the efficiency of methyl-ammonium tin iodide ($CH_3NH_3SnI_3$) based solar cells including various TCOs such as boron-doped zinc oxide (BZO), molybdenum trioxide (MoO_3) and zinc oxide (ZnO). TCO parameters such as thickness, donor concentration and operating temperature were varied to study their influence on device performance. The best device performance was achieved using MoO_3 with power conversion efficiency of 25.83 % and J_{sc}, V_{oc} and FF of 32.44 mA/cm^2, 0.979 V and 81.38 % respectively. The work shows the potential of fabricating an improved $CH_3NH_3SnI_3$ perovskite solar cell with MoO_3 as front contact.

**Corresponding author: E-mail: faruk.sani@udusok.edu.ng;*

Keywords: Boron-doped zinc oxide; efficiency; molybdenum trioxide; perovskite; zinc oxide.

1. INTRODUCTION

It is imperative to investigate an alternative energy source due to the rising of global warming caused by burning fossil fuels. The sun is the ultimate source of the most of the energy on earth. The quantity of solar radiation received by the earth in an hour is about equal to the total energy consumed by man on earth in one year [1]. Garnering the solar energy produced by the sun is a fundamental approach to attain environmentally friendly energy by direct conversion of sunlight into electricity using a device called solar cell.

Recently, organic- inorganic halide perovskites have been reported as a new material for an efficient solar cells. These new materials have totally changed photovoltaic field into the third generation solar cells. The Organic-inorganic halide perovskite solar cells have shown excellent performance from initial power conversion efficiency (PCE) of 3.8 % [2] to about 25.2 % [3]. This remarkable performance is attained due to superior properties of organic-inorganic halide perovskite; 1. High absorption co-efficient 2. High charge carrier mobility 3. Long diffusion length, 4. Direct and tunable band gap and 5. Simple methods of fabrication [4,5]. Transparent conductive oxide (TCO) with high transmittance and high conductivity has been regularly used as an essential component in perovskite solar cells. TCOs are optically transparent and electrically conductive materials. TCO must possesses a band gap ≥ 3.1 eV [6]. It was reported that TCO with high band gap transmit about 80 % of visible light [7-9].The materials that are commonly used as a TCO in perovskite solar cells are indium-doped tin oxide (ITO) and fluorine-doped tin oxide (FTO) due to their high transparency and low resistivity [10-16]. However, indium metal being rare and toxic led to the material becoming expensive and environmentally-unfriendly [17-21]. Furthermore, FTO was reported to have relatively low electrical conductivity and rigid to patterning by wet etching, and high leakage current [22].

To further explore an alternative TCO, this study investigated the role of boron-doped zinc oxide (BZO), Zinc Oxide (ZnO) and Molybdenum trioxide (MoO_3) as TCO in $CH_3NH_3SNI_3$ perovskite solar cells using SCAPS. To obtain the optimum device performance, thickness, defect density, donor density and working temperature were varied for the three different TCOs. The schematic device structure is presented in Fig. 1.

In this work, the effect of variation of thickness, defect density, donor density and working temperature of various TCOs on the performance of $CH_3NH_3SnI_3$ perovskite solar cells were investigated.

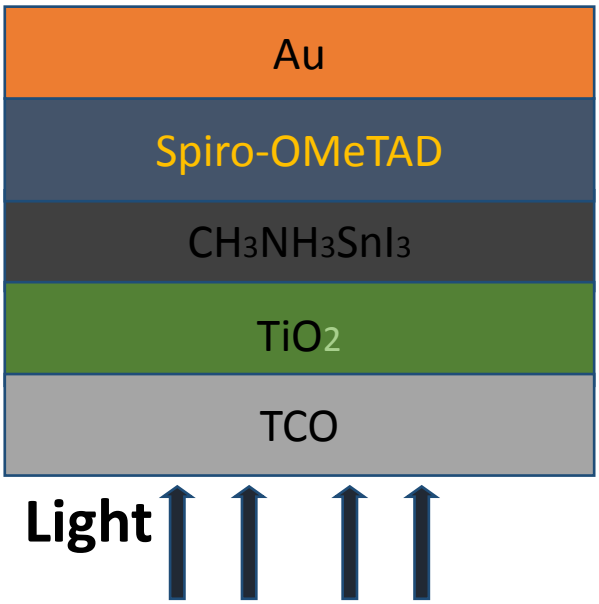

Fig. 1. Schematic presentation of tin-based perovskite solar cells

2. MATERIALSANDNUMERICAL METHOD

2.1 Materials

The materials used are TCO (BZO, ZnO and MoO_3) act as front contact, TiO_2 as Electron Transporting Material (ETM), methyl-ammonium tin iodide ($CH_3NH_3SnI_3$) as light absorbing layer, spiro-OMeTAD as Hole Transporting Material (HTM), Gold (Au) as back contact and SCAPS simulating software. The simulation parameters of those layers were obtained from previous literature [23–35] and were tabulated in Table 1. The data can be used to investigate the influence of other factors such as series and shunt resistance, defect density etc on the performance of the tin-based perovskite solar cells in planar configuration.

2.2 Numerical Method

In this study, the numerical simulation was conducted using SCAPS (SCAPS 3.3.10 version) software under AM1.5G solar illumination with an incident power density of 1000 W/cm^2, temperature 300 K, work point bias 0 V, frequency of $1.0\,X\,10^6\,Hz$ and the input parameters listed in Table 1. SCAPS is a one dimensional solar cell simulation program developed at the department of Electronics and Information Systems (ELIS) of the University of Gent, Belgium [36]. The J-V characteristics can be obtained by solving the fundamental semiconductor equations: the Poisson equations, the continuity equations for electrons and holes, and carrier transport [37]. The simulation step by step procedure is shown in Fig. 2.

3. RESULTS AND DISCUSSION

3.1 Effect of TCO on the Device Performance

The photovoltaic parameters obtained for the perovskite solar cells with the three different TCOs (BZO, ZnO, and MoO_3) are presented in Table 2 and the simulated J-V curves are plotted in Fig. 3. From Table 2, it can be seen that the device with the MoO_3 exhibits the highest PCE while the device with the ZnO acquires the lowest PCE. This shows that the undoped-ZnO has low electrical conductivity to be used as TCO. Therefore, the impurity-doped ZnO is more appropriate for TCO which is in line with the findings of [38]. The device performance with the BZO is also acceptable. The highest performance was achieved using MoO_3 with photovoltaic parameters; 0.979 V, 32.44 mA/cm^2, 81.38 % and 25.83 % for Voc, Jsc, FF, and PCE respectively. This indicates that high bandgap enables the transparent conductive oxide to transmit 80 % or more of visible light which has also been reported by [7-9]. The results obtained also show that MoO_3 has high ability than doped and undoped-zinc oxide in allowing light into the device.

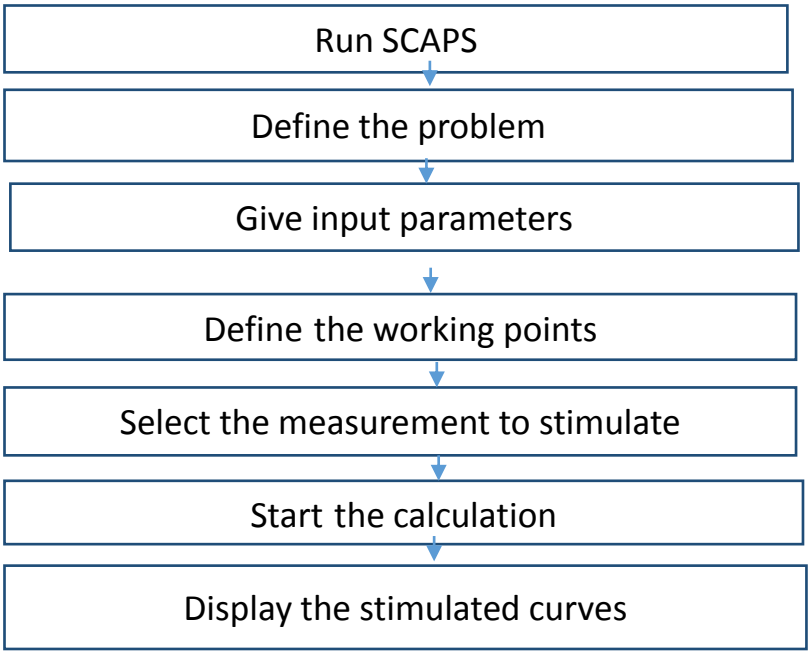

Fig. 2. SCAPS step by step procedure

Table 1. Input parameters for simulation of $CH_3NH_3SNI_3$ performance

Parameters	BZO	ZnO	MoO_3	TiO_2	$CH_3NH_3SNI_3$	Spiro-OMeTAD
Thickness (nm)	**200 (varied)**	**200 (varied)**	**200 (varied)**	**100**	**500**	**200**
E_g (eV)	3.3	3.3	3.8	3.2	1.3	3.0
X (eV)	4.55	4.6	4.1	3.9	4.17	2.45
Ɛr	9	9	9	9.0	8.2	3.0
N_c (cm^{-3})	3 x10^{18}	4 x10^{18}	2.2 x10^{18}	1 x 10^{21}	1 x 10^{18}	1 x 10^{19}
N_v (cm^{-3})	1.8x10^{19}	2 x10^{19}	1.8 x10^{19}	2 x 10^{20}	1 x 10^{18}	1 x 10^{19}
μ_n (cm^2/Vs)	100	100	30	20	1.6	0.0002
μ_p (cm^2/Vs)	31	25	6	10	1.6	0.0002
N_d (cm^{-3})	10^{20} (varied)	1x10^{17} (varied)	1x10^{17} (varied)	1 x 10^{19}	0	0
N_a (cm^{-3})	0	0	0	0	1 x 10^{16}	1 x 10^{18}
N_t (cm^{-3})	1x10^{14}	1x10^{14}	1x10^{14}	1 x 10^{15}	1 x 10^{15}	1 x 10^{15}

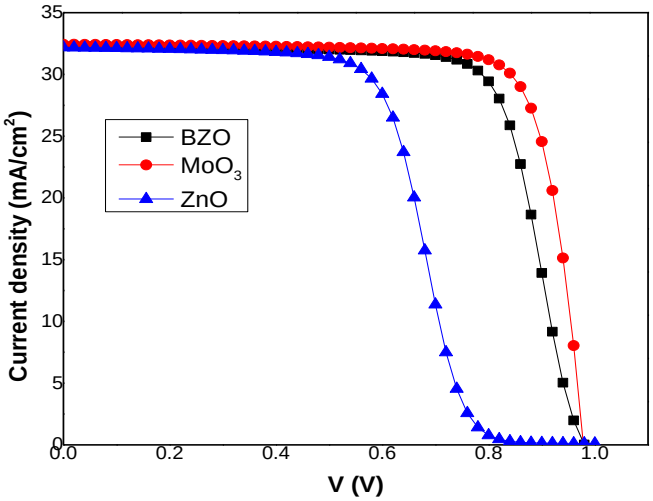

Fig. 3. Effect of different TCO on the J-V characteristics

Table 2. Photovoltaic parameters obtained using BZO, ZnO and MoO_3 as TCO

Parameters	BZO	MoO_3	ZnO
V_{oc} (V)	0.980	0.979	1.164
J_{sc} (mA/cm^2)	32.30	32.44	32.18
FF (%)	74.68	81.38	45.95
PCE (%)	23.65	25.83	17.20

3.2 Effect of TCO Thickness on the Performance of the Devices

The effect of TCO layer thickness was investigated using the numerical simulation. The thickness was varied from 300 nm to 900 nm for each of the selected TCO and the remaining input parameters remain unchanged. Fig. 4 shows the plotted J-V curves for BZO, MoO_3 and ZnO respectively. Similarly, the photovoltaic parameters obtained for BZO, MoO_3 and ZnO were tabulated in Table 2 As shown in the Tables 3 (a,b and c) there is insignificant change in the J-V characteristics. Generally, the results show that thickness of TCO could not affect the device performance.

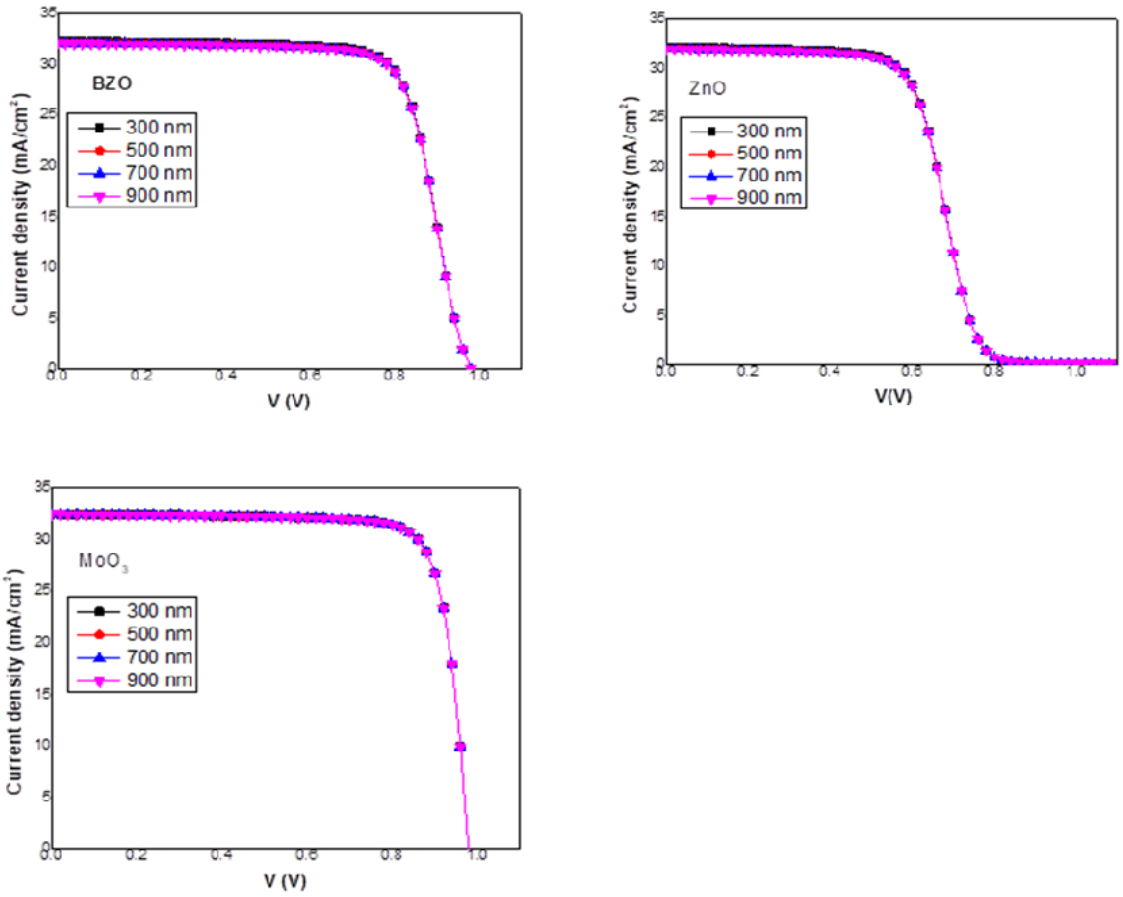

Fig. 4. Effect of TCOs thickness on the J-V characteristics

Table 3(a). Photovoltaic parameters for BZO at different thickness

Thickness (nm)	Voc (V)	Jsc (mA/cm^2)	FF (%)	PCE (%)
300	0.981	32.24	74.66	23.60
500	0.981	32.14	74.64	23.53
700	0.981	32,06	74.64	23.48
900	0.981	32.01	74.65	23.44

Table 3(b). Photovoltaic parameters for MoO_3 at different thickness

Thickness (nm)	V_{oc} (V)	J_{sc} (mA/cm^2)	FF (%)	PCE (%)
300	0.978	32.44	81.34	25.84
500	0.978	32.44	81.38	25.83
700	0.978	32.43	81.38	25.83
900	0.978	32.43	81.38	25.82

Table 3 (c). Photovoltaic parameters for ZnO at different thickness

Thickness (nm)	V_{oc} (V)	J_{sc} (mA/cm^2)	FF (%)	PCE (%)
300	1.180	32.12	45.95	17.20
500	1.198	32.03	44.60	17.12
700	1.208	31.96	44.26	17.08
900	1.213	31.91	44.06	17.06

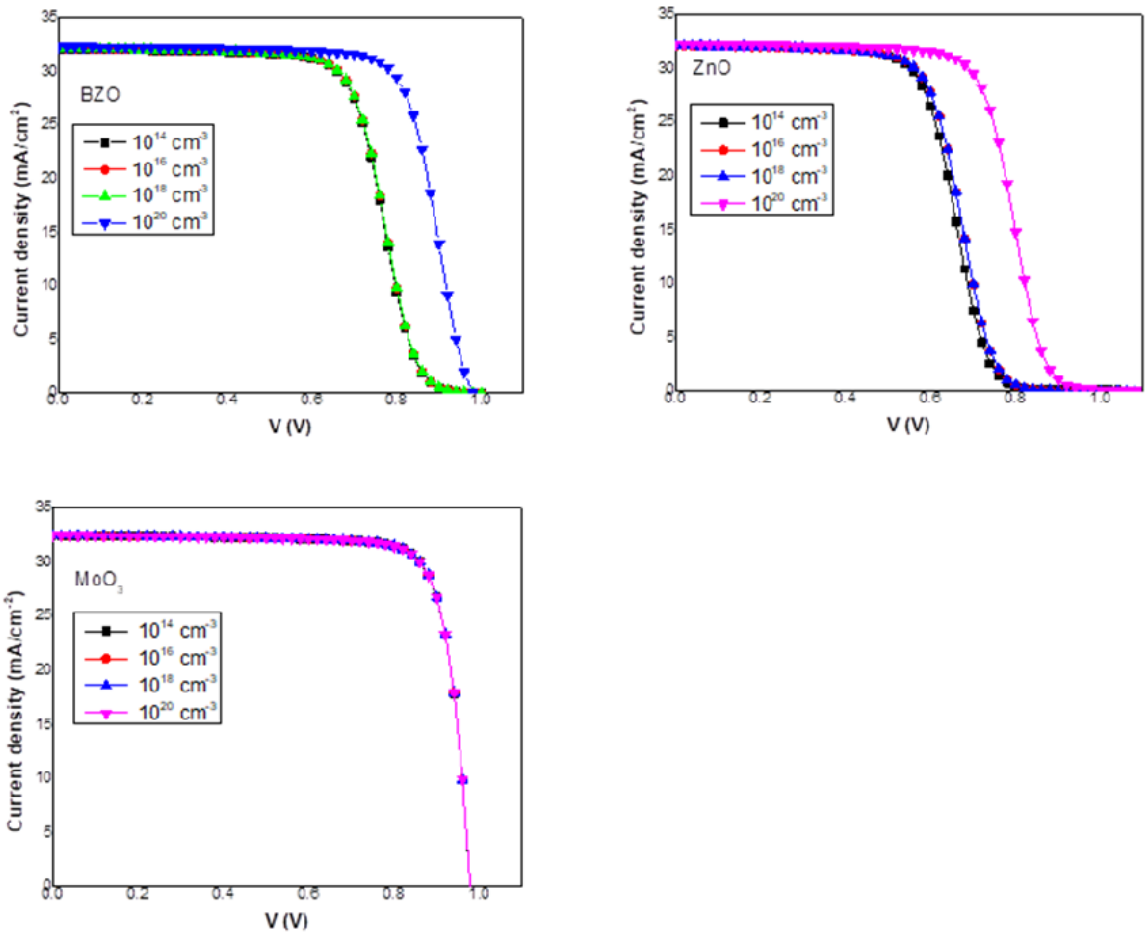

Fig. 5. Effect of TCOs layer donor density on J-V curves

Table 4(a). Photovoltaic parameters for BZO with different donor density

Parameters	10^{14} (cm^{-3})	10^{16} (cm^{-3})	10^{18} (cm^{-3})	10^{20} (cm^{-3})
V_{oc} (V)	0.987	1.047	1.107	0.980
J_{sc} (mA/cm^2)	32.10	32.16	32.26	32.30
FF (%)	62.52	59.11	58.42	74.68
PCE (%)	19.80	19.89	20.89	23.63

Table 4(b). Photovoltaic parameters for MoO_3 with different donor density

Parameters	10^{14} (cm^{-3})	10^{16} (cm^{-3})	10^{18} (cm^{-3})	10^{20} (cm^{-3})
V_{oc} (V)	0.979	0.979	0.979	0.979
J_{sc} (mA/cm^2)	32.44	32.44	32.44	32.44
FF (%)	81.36	81.38	81.38	81.38
PCE (%)	25.82	25.83	25.83	25.83

Table 4(c). Photovoltaic parameters for ZnO with different donor density

Parameters	10^{14} (cm^{-3})	10^{16} (cm^{-3})	10^{18} (cm^{-3})	10^{20} (cm^{-3})
V_{oc} (V)	1.056	1.120	1.204	1.202
J_{sc} (mA/cm^2)	32.06	32.11	32.22	32.32
FF (%)	49.86	47.59	46.10	53.39
PCE (%)	16.88	16.96	17.88	20.71

3.3 Effect of TCO Layer Donor Density

The donor density was varied from 10^{14} cm^{-3} to 10^{20} cm^{-3} and the remaining input parameters kept constant. The J-V curves for BZO, MoO_3, and ZnO are plotted in Fig. 5 Similarly, Tables 4 (a, b,c) presented the parameters attained for BZO, MoO_3, and ZnO respectively. As shown in Tables 4 (a,c) the PCE significantly increases as the donor density increase. This shows that impurity doped-zinc oxide is more suitable to be used as TCO because the electrical conductivity of undoped-zinc oxide is not sufficient enough to serve as TCO which has been suggested by [38]. Table 3 (b) illustrated that the J-V characteristics remains unchanged.

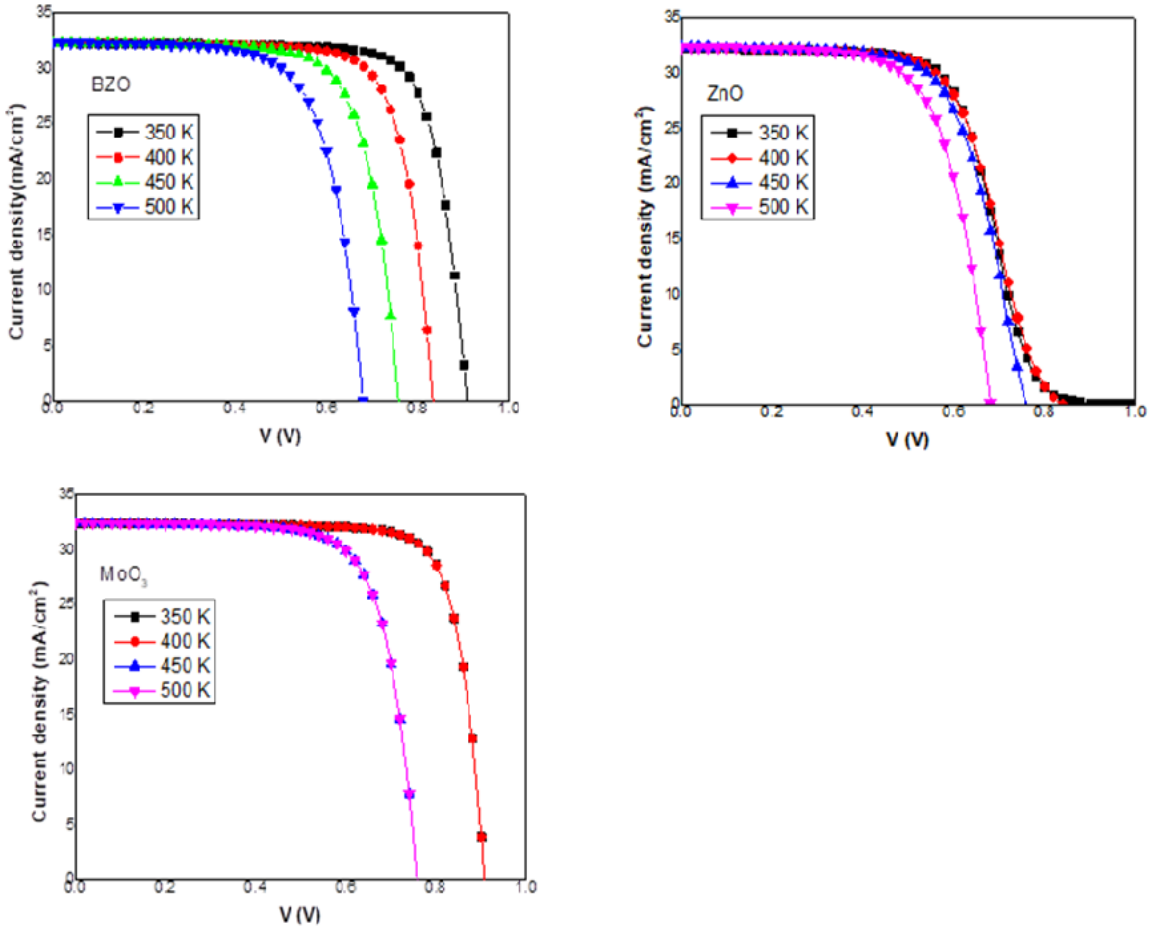

Fig. 6. Effect of TCOs temperature on the device performance

Table 5 (a). Effect of temperature on the device performance using BZO as a TCO

Parameters	350 K	400 K	450 K	500 K
V_{oc} (V)	0.907	0.834	0.758	0.680
J_{sc} (mA/cm^2)	32.32	32.33	32.33	32.31
FF (%)	78.16	78.33	73.28	69.73
PCE (%)	22.91	20.57	17.95	15.32

Table 5 (b). Effect of temperature on the device performance using MoO_3 as a TCO

Parameters	350 K	400 K	450 K	500 K
V_{oc} (V)	0.907	0.834	0.758	0.680
J_{sc} (mA/cm^2)	32.43	32.43	32.42	32.41
FF (%)	79.14	76.42	73.30	69.73
PCE (%)	23.29	20.66	18.01	15.38

Table 5 (c). Effect of temperature on the device performance using ZnO as a TCO

Parameters	350 K	400 K	450 K	500 K
V_{oc} (V)	1.043	0.841	0.759	0.680
J_{sc} (mA/cm^2)	32.25	32.30	32.34	32.37
FF (%)	50.92	62.37	66.84	67.67
PCE (%)	17.12	16.94	16.40	14.90

3.4 Effect of Operating Temperature

To study the influence of operating temperature on the device performance using three different TCO, the operating temperature was varied from 350 K to 500 K while the remaining input values remain constant. Fig. 6 shows the J-V characteristics of the perovskite solar cells using BZO, MoO_3, and ZnO respectively. The parameters obtained are tabulated in Tables 5 (a,b,c). The Tables indicate rapid decrease in power conversion efficiencies as the operating temperature increases. This might be due to decrease in V_{oc} caused by increase in operating temperature. It could be observed that there is no significant changes in J_{sc}. This reveals that J_{sc} is independent of operating temperature. Generally, the operating temperature has great impact on the cell performance. This is confirmed by our numerical study.

4. CONCLUSION

In this work, methyl-ammonium tin iodide ($CH_3NH_3SNI_3$) based solar cells including various TCOs were successively studied using SCAPS-1D simulating software. The simulation shows the influence of TCO layer thickness, donor concentration and operating temperature on the device performance. The simulation results revealed that variation of TCO thickness has no significance on the device performance. The results further show that high donor concentration improved the device performance using BZO and ZnO and achieved high efficiency at 10^{20} cm^{-3} while the cell performance remained unaffected with varied donor density using MoO_3. Also, the simulation proved that increase in temperature deteriorated the power conversion efficiency of the cell. MoO_3 exhibited best PCE of 25.83 % in contrast to BZO and ZnO with PCE of 23.65 % and 17.20 % respectively. It can be concluded that MoO_3 is a potential alternative TCO layer in perovskite solar cells.

COMPETING INTERESTS

Authors have declared that no competing interests exist.

REFERENCES

1. Musa AO. Principles of Photovoltaic Energy Conversion. Published by A.B.U Press Limited, Zaria, Kaduna State, Nigeria; 2010.
2. Kojima A, Teshima K, Shirai Y, Miyasaka, T. Organometal Halide Perovskites as Visible- Light Sensitizers for Photovoltaic Cells. Journal of American Chemical Society. 2009;131:6050–6051.
3. nrel-research-pushes-perovskites-closer-to-market@ Available:www.nrel.gov.https://www.nrel.gov/news/program/2021/new-perovskite-design-shows-path-to-higher-efficiency.html (Retrieved May 25, 2021).
4. Chen Q, Marco ND, Yang Y, Song TB, Chen CC, Zhou H, Yang Y. Under the Spotlight: The Organic-Inorganic Hybrid Halide Perovskite for Optoelctronic Applications. Nano Today. 2015; 10:355-396.
5. Green. MA, Ho-Baillie A, Snaith HJ. The emergence of perovskite solar cells. Nature Photonics. 2014;8(7):506–514.
6. Guillén, C. and Herrero, J. (2011). TCO/metal/TCO structures for energy and flexible electronics. Thin Solid Films 520, 1–17. Available:http://dx.doi.org/10.1016/j.tsf.2011.06.091.
7. Bawaked SM, Sathasivam S, Bhachu DS, Chadwick N, Obaid AY, Al-Thabaiti S, Basahel SN, Carmalt CJ, Parkin IP. Aerosol assisted chemical vapor deposition of conductive and photocatalytically active tantalum doped titanium dioxide films. J. Mater. Chem. A 2014;2:12849. Available:http://dx.doi.org/10.1039/C4TA01618A.
8. Bhachu DS, Sankar G, Parkin IP. Aerosol assisted chemical vapor deposition of transparent conductive zinc oxide films. Chem. Mater. 2012;24:4704–4710. Available:http://dx.doi.org/10.1021/cm302913b

9. Sathasivam S, Bhachu DS, Lu Y, Chadwick N, Althabaiti SA, Alyoubi AO, Basahel SN, Carmalt CJ, Parkin IP. Tungsten doped TiO2 with enhanced photocatalytic and optoelectrical properties via aerosol assisted chemical vapor deposition. Sci. Rep. 2015;5:10952. Available:http://dx.doi.org/10.1038/srep10952.
10. Noel NK, Stranks SD, Abate A, Wehrenfennig C, Guarnera S, Haghighirad A-A, Sadhanala A, Eperon GE, Pathak SK, Johnston MB. Lead-free organic–inorganic tin halide perovskites for photovoltaic applications. Energy Environ. Sci. 2014;7:3061–3068.
11. Hao F, Stoumpos CC, Cao DH, Chang RP, Kanatzidis MG. Lead-free solid-state organic–inorganic halide perovskite solar cells. Nat. Photonics 2014;8:489.
12. Hao F, Stoumpos CC, Guo P, Zhou N, Marks TJ, Chang RP, Kanatzidis MG. Solvent-mediated crystallization of $CH_3NH_3SnI_3$ films for heterojunction depleted perovskite solar cells. J. Am. Chem. Soc. 2015;137:11445–11452.
13. Yokoyama, T, Cao DH, Stoumpos CC, Song T-B, Sato Y, Aramaki S, Kanatzidis MG. Overcoming short-circuit in lead-free $CH_3NH_3SnI_3$ perovskite solar cells via kinetically controlled gas–solid reaction film fabrication process. J. Phys. Chem. Lett. 2016;7:776–782
14. Fujihara T, Terakawa S, Matsushima T, Qin, C, Yahiro, M, Adachi, C. Fabrication of high coverage $MASnI_3$ perovskite films for stable, planar heterojunction solar cells. J. Mater. Chem. C. 2017;5:1121–1127.
15. Yu, Y, Zhao, D, Grice, CR, Meng W, Wang C, Liao, W, Cimaroli, AJ, Zhang, H, Zhu, K, Yan Y. Thermally evaporated methylammonium tin triiodide thin films for lead-free perovskite solar cell fabrication. RSC Adv. 2016;6:90248–90254.
16. Peng L, Xie W. Theoretical and experimental investigations on the bulk photovoltaic in lead-free perovskites $MASnI_3$ and $FASnI_3$. RSC Adv. 2020;10:14679–14688.
17. Dianetti M, Di Giacomo F, Polino G, Ciceroni, C, Liscio, A, D'Epifanio A, Licoccia S, Brown, TM, Di Carlo A, Brunetti F. TCO-free flexible organo metal trihalide perovskite planar-heterojunction solar cells. Sol. Energy Mater. Sol. Cells, 2015;140:150–157.
18. Hagendorfer, H, Lienau K, Nishiwaki S, Fella, CM, Kranz, L, Uhl AR, Jaeger D, Luo L, Gretener, C, Buecheler S, Romanyuk YE, Tiwari AN. Highly transparent and conductive ZnO: Al thin films from a low temperature aqueous solution approach. Adv. Mater. 2014;26:632–636.
19. Minami T. Transparent conducting oxide semiconductors for transparent electrodes. Semicond. Sci. Technol. 2005;20:S35–S44.
20. Sibin´ ski, M., Znajdek K, Walczak S, Słoma, M, Górski M, Cenian A. Comparison of ZnO:Al, ITO and carbon nanotube transparent conductive layers in flexible solar cells applications. Mater. Sci. Eng. B Solid-State Mater. Adv. Technol. 2012;177:1292–1298.
21. Sohn, S., Kim, H. Transparent conductive oxide (TCO) films for organic light emissive devices (OLEDs). Org. Light Emit. Diode – Mater. Process Dev. 2011;233–274
22. Liu H, Avrutin, V., Izyumskaya, N., Özgr, Ü., Morkoç, H. Transparent conducting oxides for electrode applications in light emitting and absorbing devices. Superlatt. Microstruct. 2010; 48:458–484.
23. Patel PK. Device simulation of highly efficient eco-friendly $CH_3NH_3SnI_3$ perovskite solar cell. Scientific reports. 2012;11:3082 DOI:10.1038/s41598-021-828-w
24. Baig F, Khattak YH, Marí B, Beg, S, Ahmed, A, Khan K. Efficiency Enhancement of CH3NH3SnI3 Solar Cells by Device Modeling. J. Electron. Mater. 2018;47:5275 5282.
25. Azri F, Meftah A, Sengouga N, Meftah A. Electron and hole transport layers optimization by numerical simulation of a perovskite solar cell. Sol. Energy. 2019;181:372-378.
26. Minemoto T, Murata M. Impact of work function of back contact of perovskite solar cells without hole transport material analyzed by device simulation. Curr. Appl. Phys. 2014;14:1428–1433.
27. Teimouri R, Mohammadpour, R. Potential application of CuSbS 2 as the hole transport material in perovskite solar cell: A simulation study. Superlattices Microstructure. 2018;118: 116–122.
28. Slami A, Bouchaour. M, Merad. L. Comparative Study of Modelling of Perovskite Solar Cell with Different HTM Layers. International Journal of Materials. 2020;7.

29. Bedia, FZ, Bedia A, Aillerie, M, Maloufi N, Genty, F, Benyocef, B. Influence of Al-doped ZnO transparent contacts deposited by a spray pyrolysis technique on performance of HIT solar cells. Energy procedia, 2014;(50):853-861, doi: 10.1016/j.egypro.2014.06.104.
30. Raudik SA, Mozharov AM, Mitin DM, Bolshakov AD, Rajanna PM, Nasibulin AG, Mukhin IS. Numerical simulation of the carbon nanotubes transport layer influence on performance of GaAs solar cells. IOP conf. series: Journal of physics; 2018. DOI: 10.1088/1742-6596/1124/4/041040
31. Baba BJ, Mandapu U, Vedanayakam V, Tyagarajan K. Optimization of high efficiency tin halide perovskite solar cells using SCAPS-1D. International journal of simulation and process modelling, 2018;13(3):221, DOI: 10.150/IJSPM.2018.10014179.
32. Rahman, MA. Design and simulation of a high performance Cd-free Cu2SnSe3 solar cells with SnS electron-blocking hole transport later by SCAPS-1D. SN Applied sciences. 2021;3253. DOI: 10.1007/s42452-021-04267-3.
33. [Ouedraogo S, Zougmore F, Ndjaka JM. Numerical analysis of copper-indium-Gallium-Diselinide-based solar cells by SCAPS-1D. International Journal of Photoenergy. 2013;421076:9. DOI: 10.1155/2013/421076.
34. Zaid B, Ullah MS, Hadjoudja B, Gagui S. Role of TC films in improving the efficiency of Cds/MoS2 heterojunction solar cells. Journal of Nano and Electronic Physics. 2019;11(2): 02030 DOI: 10.21272/jnep.11(2).02030.
35. Mozafari, B, Shahhoseini. Using Molybdenum trioxide as a TCO layer to improve performance of CdTe/CdS thin film solar cell. Signal processing and Renewable Energy. 2020;57-65.
36. Burgelman M, Decock K, Niemegeers A, Verschraegen J, Degrave S. SCAPS Manual, Department of Electronics and Information System (ELIS), University of Gent, Belgium; 2012.
37. Movla H. Optimization of the CIGS based thin film solar cells: numerical simulation and analysis. Optik. 2014;125(1):67–70.
38. Chen J, Chen D, Zhou Y, Li W, Yanjie R, Hu L. Electrochemical deposition of Al-doped ZnO transparent conducting nanowires arrays for thin-film solar cell electrodes. Mater. Lett. 2014; 117:162-164.

Peer-review history:
The peer review history for this paper can be accessed here:
https://www.sdiarticle4.com/review-history/73049